

Article

Mineral Characteristics and the Mineralization of Leptynite-Type Nb–Ta Ore Deposit in the Western Qilian Orogenic Belt

Junpeng Yu ^{1,2}, Yibu Wu ^{2,*}, Chunhui Zhang ¹, Haojia Si ², Dongze Si ² and Chengjun Zhang ^{1,*}

¹ Key Laboratory of Mineral Resources in Western China, College of Earth Sciences, Lanzhou University, Lanzhou 730000, China

² Geological Survey of Gansu Province, Lanzhou 730050, China

* Correspondence: ttwyb123@163.com (Y.W.); cjzhang@lzu.edu.cn (C.Z.)

Abstract: A large Nb–Ta ore deposit was found in the Yushishan leptynite in the west Qilian Orogenic Belt (QOB). Based on a field geological survey and using a Mineral Liberation Analyser (MLA), including scanning electron microscopy (SEM) and energy-dispersive spectrometer (EDS) methods, eight Nb minerals (fergusonite, polycrase, columbite, Nb-rutile, aeschynite, pyrochlore, microlite, and ilmenorutile) were found to occur in the leptynite. This accounted for approximately 69% of Nb, with fergusonite, polycrase, and columbite being the dominant phases. The other 17.90% Nb as a minor element was dispersed in titanium magnetite–maghemite, and another 13.00% Nb was dispersed in gangue minerals. Nb minerals are formed mainly by two metallogenesis stages. The first stage is magmatic genesis to form four Nb minerals, euhedral-subhedral fergusonite, polycrase, pyrochlore, and microlite, which are crystallized within or between primary minerals, such as quartz and feldspar. Late alteration phenomena are locally observed. The second stage is the hydrothermal genesis of columbite, anhedral fergusonite, Nb-rutile, and aeschynite, which are dispersed in the fissures of the wall rocks as irregular veins and lump assemblages. Meanwhile, they are closely associated with metasomatic chlorite, albite, and secondary quartz. Furthermore, direct metasomatism among different Nb minerals is also found at the local scale. The Nb percentage of these two Nb mineral mineralization types is approximately equal, which reflects two main mineralizing periods. The first stage of mineralization occurred in the Neoproterozoic Era (834–790 Ma). Magmatism of this period produced early niobium and formed fergusonite, polycrase, pyrochlore, microlite, and zircon. The initial enrichment of Nb, Ta, and other rare metals occurred during this stage. The second stage of mineralization occurred in the Caledonian period (490–455 Ma). Large-scale and intense tectonic-magmatic thermal events occurred in the western part of the QOB due to the plate subduction and convergence (510–450 Ma). Hydrothermal activity in this period formed columbite, fergusonite, Nb-rutile, and aeschynite. Moreover, rare metal elements in the Nb-bearing rocks activated and migrated at short distances, forming in situ Nb–Ta-rich ore deposits.



Citation: Yu, J.; Wu, Y.; Zhang, C.; Si, H.; Si, D.; Zhang, C. Mineral Characteristics and the Mineralization of Leptynite-Type Nb–Ta Ore Deposit in the Western Qilian Orogenic Belt. *Minerals* **2023**, *13*, 218. <https://doi.org/10.3390/min13020218>

Academic Editor: Stefano Salvi

Received: 13 December 2022

Revised: 29 January 2023

Accepted: 30 January 2023

Published: 2 February 2023

Keywords: Nb–Ta minerals; leptynite type deposit; metallogenetic model; Yushishan; Qilian Orogenic Belt (QOB)

1. Introduction

Niobium (Nb) and tantalum (Ta) are strategic rare metal elements. They have high heat resistance, melting point, ductility, corrosion resistance, and thermal conductivity. They are important raw materials for electronics, atomic energy, aerospace, iron and steel, chemistry, and other industries [1–4]. Furthermore, they are irreplaceable in national defense, energy, high-tech, and medical fields. Nb–Ta ore deposits can be hosted in igneous or in sedimentary rocks [5], and the magmatic deposits are the most important. Magmatic Nb–Ta ore deposits can be divided into pegmatitic [6–9], granitic [10–14], alkaline [15–18], and carbonatite types [19–22]. Sedimentary Nb–Ta ore deposits are mainly formed in

 **Copyright:** © 2023 by the authors. Licensee MDPI, Basel, Switzerland. This article is an open access article distributed under the terms and conditions of the Creative Commons Attribution (CC BY) license (<https://creativecommons.org/licenses/by/4.0/>).

weathering crusts and sedimentary strata [23]. Some researchers posit that Nb and Ta are gradually enriched during fractional crystallization processes [24–29], and others claim that they are formed by hydrothermal and metasomatic processes associated with late stages of magmatic activity [30–32]. Moreover, there are some researchers who believe that it is a mixed genesis [33,34].

The Yushishan deposit is a large Nb-Ta ore deposit that was discovered in the western part of the central Qilian Mountains. It is a strata-bound ore deposit formed in the Precambrian metamorphic leptynite horizon [35–37]. The geological characteristics, protolith, and age of mineralization of the deposit have been studied previously [35–43]. Jiang et al. (2022) conducted a series of studies on the deposit [37]. They mainly discussed the geochemical characteristics of leptynite, the diagenetic age, the characteristic of the Nb-Ta orebodies, and the ore genetic model of the Yushishan Nb-Ta deposit [37]. However, ore minerals containing Nb, Ta, and other rare metal elements in this deposit have not been studied in detail. Therefore, there are still open questions. On the one hand, the species and genesis of Nb mineral and Nb-bearing minerals in the Nb-Ta ore deposit are poorly understood [36,40]. On the other hand, the occurrence mode of Nb in the ore rocks and mineral-disseminated properties have not been systematically studied. Moreover, deposit genesis and metallogenetic types are still debated to date [37,40,41,44,45]. Initially, we analyze the compositions of Nb-Ta ore bodies and species of Nb minerals and Nb-bearing minerals in this study. Next, the paragenetic properties of Nb-Ta minerals are analyzed in detail. In addition, the occurrence mode of Nb and the genesis of Nb minerals are discussed. Finally, we introduce the metallogenetic type of Yushishan Nb-Ta ore deposit. Our study provides a reference for leptynite-type Nb-Ta ore deposit exploration.

2. Geological Setting

The Yushishan Nb-Ta ore deposit is located at the intersection of the Tarim and Qaidam Blocks (Figure 1A). With the boundary along the Altun Tagh fault, the northern and southern parts are the Northern Altun Tagh Block and Quanji Block in the northern Qaidam Basin (also referred to as the Oulongbuluke Block), respectively; the western and eastern parts are the Hongliugou–Lapeiquan Ophiolite Belt and the central and Southern Qilian Arc–Basin system, respectively. The main body is located in the western part of the QOB. These areas have undergone multi-cycle orogenic activities since the Pre-Caledonian, Caledonian, and Himalayan periods. The geological bodies formed under different geneses, ages, and tectonic environments were assembled in rock and fault blocks during the long-term geological evolution. Thus, modern complex tectonic patterns and abundant mineral resources were formed [46–50].

The exposed strata in this area are the Paleoproterozoic Dakendaban Group (Pt_1D), the Aoyougou Formation (Ch_a) in the Statherian–Calymmian period, the Binggounan Formation ($JxQbb$) in the Ectasian–Stenian period, the Cambrian–Ordovician Lapeiquan group (ϵOL_p), and the Carboniferous–Permian (CPy) Yingeblik Formation [38]. The Yushishan Nb-Ta ore deposit is hosted by the Aoyougou formation (Figure 1).

Magmatic activity in this region mainly occurred in the Caledonian, followed by the Variscan and Yanshanian. Intermediate-felsic magmatic rocks formed as stocks or dykes. The wall rocks of the Yushishan Nb-Ta ore deposit are mainly monzonitic granite and then tonalite.

The regional tectonic setting is very complex in this area. A series of the east–westward, north–east–eastward, and north–west–westward, mainly translation fault systems, were formed under multi-stage tectonic activities of the Altun Tagh Great Fault and other faults.

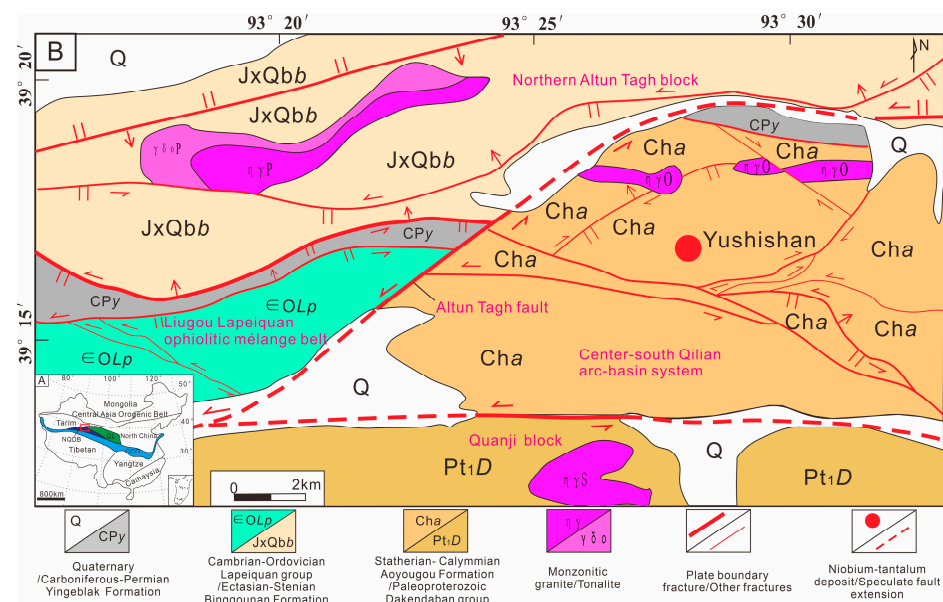


Figure 1. Geotectonic location of the Yushishan area (A) and geological ore deposit sketch map (B) [37,38]. QL, Qilian block; CCO, Central China Orogeny; NQDB, North Qaidam continental-type UHPM belt.

3. Geological Characteristics of the Ore Deposit

3.1. Geological Features of the Mine Site

The main Nb-Ta hosting unit is the Aoyougou Formation (Cha), which extends west-northwest to the east-northeast. Due to the strong tectonic transformation, the horizon from north to south is a set of amphibolite-leptynite-marble assemblages (Figure 2). Leptynite is the host rock of Nb-Ta. The main granite body exposed in the mine area is Ordovician diorite granite (Figure 2), which intruded into the strata of the Aoyougou Formation. It formed at approximately 481.3 ± 1.7 Ma in the early Ordovician period [42]. Contact with the wall rocks is relatively secant and sometimes undulated. Some enclosure edges are enriched with felsic minerals. The wall rock xenoliths become more abundant towards the margins of the intrusion. The monzonitic granite is characterized as high in silica, alkali-rich, and Fe–Mg–Ca-rich. It is I-type granite within the potassium basaltic quasi-aluminous to weak peraluminous series [42]. There are three types of faults in the study area, high-angle reverse fault (dip $> 45^\circ$), reverse strike-slip fault (dip $> 45^\circ$), and strike-slip fault.

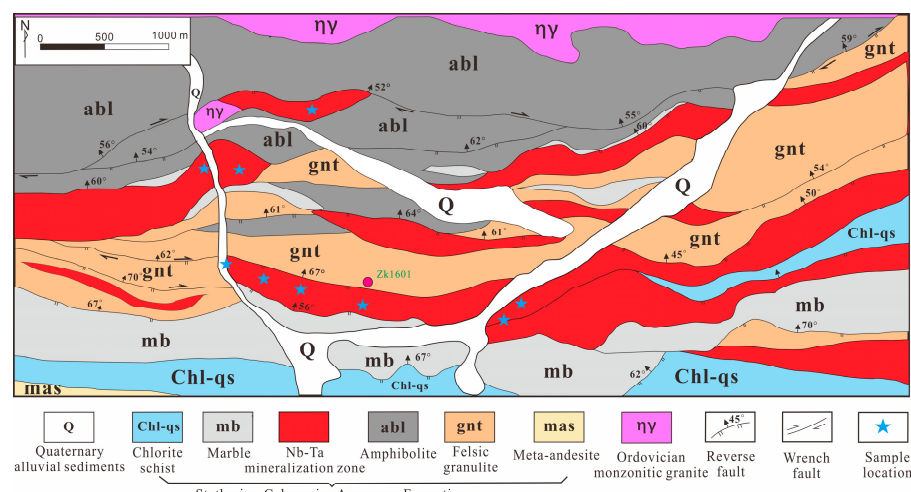


Figure 2. Geological map of Yushishan Nb-Ta ore deposit and sample sites.

3.2. Orebody Characteristics

The Nb-Ta mineralized zone is spread along the east–western direction and was formed as layers in the leptynite of the Aoyougou Formation (Figures 2 and 3). It shows a trend of slight divergence to the east and convergence to the west. The length is greater than 10 km, and the width is approximately 3 km from north to south. The Nb-Ta mineralized zone is strata-bound. Both orebody sides are strictly controlled by faulted contacts with marble (Figure 3). In total, 29 ore bodies were identified. The ore bodies were produced along the layers in laminar or plate-like organization. The ore bodies are 534–2826 m in length and 7.88–37.84 m in thickness. The average ore grade of $(\text{Nb}, \text{Ta})_2\text{O}_5$ is 0.060%–0.313%, and the associated rare earth oxide (RE_2O_3) content is 0.20%–0.64%.

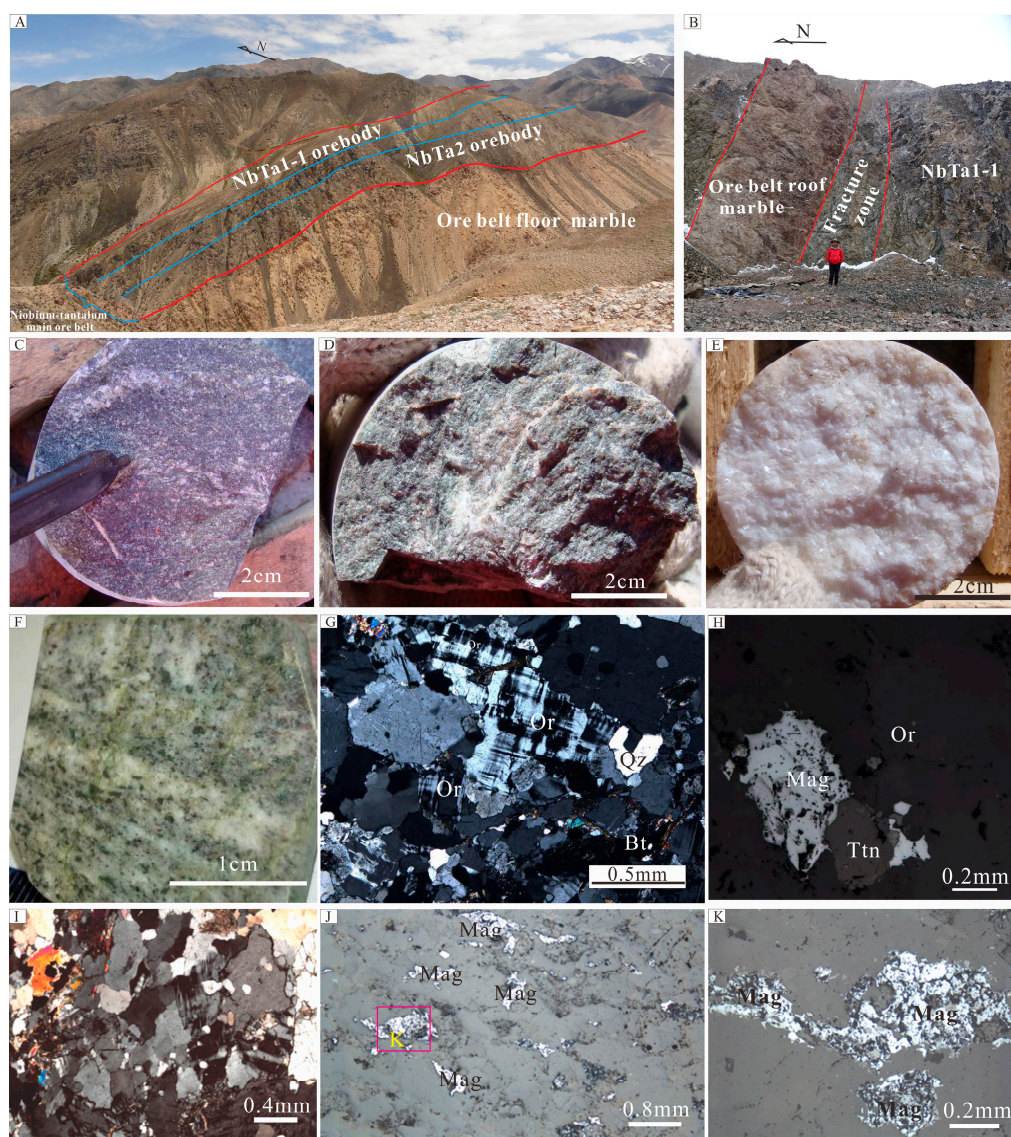


Figure 3. Yushishan Nb-Ta ore belt, ore body, and ore characteristics (Or, orthoclase; Ttn, titanite; Mag, magnetite; Qz, quartz; Bt, biotite). (A) The main Nb-Ta ore belt and ore body in Yushishan. (B) The marble roof contact surface in the northern side of the ore belt. The roof and floor of the ore belt is dolomite marble, and the ore belt and dolomite marble are in fault contact. (C–E) Nb-Ta ore of plagioclase leptynite-type, monzonite leptynite-type, and medium-grain-size dolomite marble of floor in the borehole ZK1601. (F–H) Leptynite-type ore (black minerals are mainly magnetite; anhedral granular quartz, subhedral–anhedral granular orthoclase, plagioclase biotite, and microcline in the rocks). (I–K) Plagioclase granitic ore.

The main hosting rocks are plagioclase leptynite and monzonitic leptynite (Figure 3C,D,F). The main minerals are quartz, plagioclase, and orthoclase, followed by chlorite, muscovite, biotite, titanite, and magnetite (Figure 3F). The metallic minerals observed with the naked eye are mostly magnetite (Figure 3F). The grain size of magnetite is mostly less than 0.2 mm and occurs as vein-like, irregular agglomerate, and disseminated forms (Figure 3H,J,K). The paragenetic relationship between fergusonite and magnetite can be observed using scanning electron microscopy (SEM) (Figure 3K).

4. Methods

The industrial grade of Nb-Ta rare metal deposit is on the order of magnitude of 10^{-6} . A large number of samples need to be collected in order to reach the industrial grade of the deposit. Moreover, minerals with extremely low content also need to be enriched by beneficiation with a large number of samples. Meanwhile, fresh high-, medium-, and low-grade samples were collected from 9 different parts of the niobium-bearing leptynite ore body to ensure the representativeness of the samples. All the samples weigh approximately 5035 kg. Parts of the samples were identified by rock slices and analyzed by SEM. The others were crushed and mixed. Then, the mixed samples are divided into three categories: Mineral Liberation Analyser (MLA) determination samples, assay analysis samples, and beneficiation experimental samples. After the samples were beneficiated and analyzed with MLA, the results of some minerals with extremely low content reached four decimal digits. Mineral species were determined based on the MLA method. At the same time, the mineral composition, structure, and disseminated characteristics were tested using the FEI MLA650 mineral automatic analysis system, which includes an FEI QUANTA650 (The Natural History Museum, London, UK) scanning electron microscope with a 3 nm resolution and a BRUKER (Billerica, MA, USA) XFlash5010 energy spectrometer with a 0.5–1 μm small beam spot. The MLA test conditions were an SEM operating voltage of 20 kV, working distance of 10.0 mm, and beam spot of 7.0 μm . The experimental error is $\pm 10^{-4}$ for the mineral percentage. The experiments were conducted at the Guangzhou Institute of Non-ferrous Metals.

In this study, the slice grain size method was used to measure the mineral grain size. Under the microscope, the diameter of grains in the slices was measured, and the percentage of grains in each group was calculated at 1/4 intervals. More than 300 grains were counted in each slice. The error was $\pm 1 \mu\text{m}$.

5. Results

5.1. Mineral Species of the Nb-Ta Ore Deposit

The results of MLA quantitative analyses carried out on the gangue minerals of the Nb-Ta ore deposit showed that they were composed of quartz (40.7989 wt.%), orthoclase (26.4793 wt.%), plagioclase (17.0338 wt.%), chlorite (5.0442 wt.%), muscovite (3.5596 wt.%), calcite (0.6195 wt.%), and biotite (0.4048 wt.%). The Nb-Ta minerals were Nb-rutile, fergusonite, polycrase, columbite, trace aeschynite, pyrochlore, microlite, and ilmenorutile. There were differences in the contents of Nb, Fe, and Ti between ilmenorutile and Nb-rutile, as well as in the structure. The chemical formulae of ilmenorutile and Nb-rutile are $(\text{Ti},\text{Nb},\text{Ta},\text{Fe})\text{O}_2$ and TiO_2 , respectively. The contents of Nb_2O_5 in ilmenorutile and Nb-rutile are 5.10%–26.52% and 0.38%–2.88%, respectively; the rare earth mineral contents are synchysite, bastnaesite, parisite, monazite, xenotime, allanite, and yttrium hinganite; the Zr-bearing mineral is zircon; and the iron-titanium oxide minerals are magnetite/magnetite hematite, limonite, and ilmenite (Table 1).

Table 1. Quantitative analysis results of minerals in ores.

Mineral	Empirical Formula	Content (wt.%)	Mineral	Empirical Formula	Content (wt.%)	Mineral	Empirical Formula	Content (wt.%)
Ilmenorutile	(Ti,Nb,Ta,Fe)O ₂	0.0028	Yttrium hinganite-(Y, Ce, Yb)	(Y,Ce,Yb)BeSiO ₄ (OH)	0.0014	Ankerite	Ca(Mg,Fe)[CO ₃] ₂	0.1297
Nb-Rutile	TiO ₂	0.1817	Zircon	ZrSiO ₄	0.4164	Kutnohorite	CaMn[CO ₃] ₂	0.0247
Fergusonite	YNbO ₄	0.0248	Quartz	SiO ₂	40.7989	Magnetite-maghemite	Fe ²⁺ Fe ³⁺ O ₄ -Fe ₂ O ₃	3.7450
Polycrase	YNb ₂ O ₆	0.0231	Plagioclase	Na[AlSi ₃ O ₈]-Ca[Al ₂ Si ₂ O ₈]	17.0338	Limonite	α -FeO(OH)-nH ₂ O	0.6520
Columbite	(Fe, Mn)(Nb, Ta) ₂ O ₆	0.0126	Orthoclase	KAlSi ₃ O ₈	26.4793	Ilmenite	FeTiO ₃	0.1117
Aeschynite	Ca ₂ Fe ²⁺ (Ti,Nb, Fe ³⁺) ₂ O ₆	0.0066	Muscovite	KAl ₂ [AlSi ₃ O ₁₀](OH) ₂	3.5596	Titanite	CaTi[SiO ₄]O	0.0130
Pyrochlore	(Ca,Na) ₂ Nb ₂ O ₆ (OH,F)	0.0032	Biotite	K(Mg,Fe) ₃ [Si ₃ AlO ₁₀ (OH) ₂]	0.4048	Apatite	Ca ₅ [PO ₄] ₃ (F,Cl,OH)	0.0624
Microlite	(Ca,Na) ₂ (Ta,Nb) ₂ O ₆ (O,OH,F)	0.0024	Epidote	Ca ₂ (Al,Fe) ₃ [SiO ₄][Si ₂ O ₇](OH) ₂	0.0886	Prehnite	Ca ₂ Al[AlSi ₃ O ₁₀](OH) ₂	0.0008
Synchysite-(Ce)	CaCe[CO ₃] ₂ F	0.0903	Psilomelane	BaMn ²⁺ Mn ⁴⁺ O ₂₀ ·3H ₂ O	0.0327	Pyrite	FeS ₂	0.0109
Bastnaesite-(Ce, La)	(Ce,La)[CO ₃](F,OH)	0.0689	Actinolite	Ca ₂ (Mg,Fe) ₅ [Si ₄ O ₁₁] ₂ (OH) ₂	0.0444	Barite	BaSO ₄	0.0006
Parisite-(Ce)	CaCe ₂ [CO ₃] ₃ F ₂	0.0460	Kaolinite	Al ₄ [Si ₄ O ₁₀](OH) ₈	0.0160	Chromite	FeCr ₂ O ₄	0.0082
Monazite-(La, Ce)	(Ce,La)[PO ₄] ₄	0.0173	Chlorite	(Mg,Al,Fe) ₆ [(Si,Al) ₄ O ₁₀](OH) ₈	5.0442	Other		0.0675
Allanite-(Ce, La, Y)	Ca,Mn,Ce,La,Y,Th) ₂ (Fe ²⁺ ,Fe ³⁺ ,Ti)(Al,Fe) ₂ [Si ₂ O ₇] ₂ [SiO ₄]O(OH)Y[PO ₄]	0.0142	Fluorite	CaF ₂	0.1338	Total		100.0000
Xenotime-(Y)		0.0062	Calcite	CaCO ₃	0.6195			

5.2. Mineralogical Properties and Dissemination Characteristics of Nb Minerals

5.2.1. Grain Size of the Main Minerals

The grain size analysis of Nb minerals showed that the Nb minerals are generally fine in size, less than 160 μm . The grain size of most Nb minerals is below 80 μm . The percentages of polycrase and pyrochlore with grain sizes between 80 and 160 μm are 10.12% and 9.73%, respectively (Table 2). The percentages of fergusonite, polycrase, and columbite with grain sizes between 10 and 160 μm are 79.36%, 69.29%, and 77.80%, respectively (Table 2). In addition, the percentages of pyrochlore, microlite, and rutile with grain sizes between 10 and 160 μm are 88.31%, 32.34%, and 42.32%, respectively (Table 2).

Table 2. Measurement results of grain size of the main Nb minerals.

Grain Size/ μm	Grain Size Distribution of Mineral/Grain Volume%					
	Fergusonite	Polycrase	Columbite	Pyrochlore	Microlite	Nb-Rutile
80–160		10.12		9.73		
40–80	7.29	17.87	14.40	19.99	5.93	
20–40	37.67	22.15	33.46	38.62	9.95	14.25
10–20	34.40	19.15	29.94	19.97	16.46	28.07
5–10	16.17	18.95	16.19	8.20	26.78	34.49
<5	4.47	11.76	6.01	3.49	40.88	23.19
Total	100.00	100.00	100.00	100.00	100.00	100.00

5.2.2. Mineralogical Properties and Dissemination Characteristics of Main Ores

Fergusonite is the most abundant Nb mineral in this ore, with a mineral content of 0.0248 wt.%. Fergusonite in the ore is euhedral–subhedral or anhedral granular with complex dissemination characteristics. Its grain size is mainly between 5 and 80 μm . There are four main types of textures (Figure 4): (1) the fergusonite crystal is relatively complete and disseminated into orthoclase and quartz in euhedral fine-grained crystal, often crystallizing at the same time as zircon (Figure 4A–C); (2) the euhedral fine-grained fergusonite crystallize at the same time as magnetite or is included in magnetite (Figure 4D,E); (3) anhedral granular fergusonite and columbite are deposited as irregular aggregates in quartz fissures and are associated with zircon (Figure 4F); (4) anhedral granular fergusonite is included in

columbite and at the edge of the fine albite veins. The anhedral granular fergusonite, albite, and columbite are hosted in the orthoclase fissures (Figure 5E).

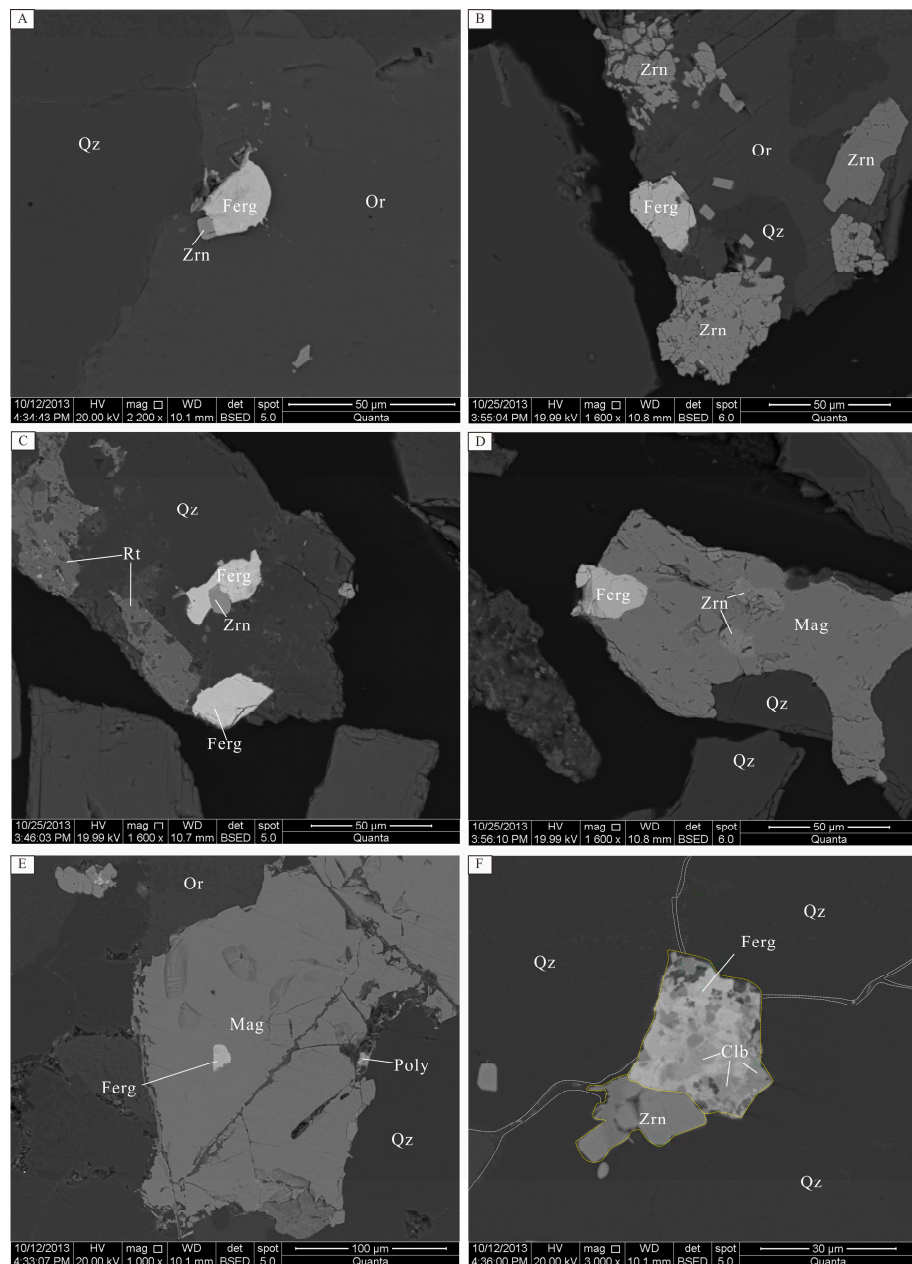


Figure 4. The dissemination characteristics of fergusonite in ores and an SEM BSE image (Ferg, fergusonite; Or, orthoclase; Qz, quartz; Zrn, zircon; Mag, magnetite; Clb, columbite; Poly, polycrase). (A) Euhedral fergusonite intergrown with zircon disseminated in the super-fine grains of orthoclase. (B) Euhedral fergusonite intergrown with zircon disseminated in the micro-fine grains of orthoclase. (C) Euhedral fergusonite intergrown with zircon disseminated in the micro-fine grains of quartz. (D) Euhedral fergusonite disseminated in magnetite intergrowths with zircon. (E) Euhedral fergusonite is contained in magnetite in the state of fine particles. (F) Fergusonite and columbite aggregate and exhibit intergrowth with zircon. Moreover, all of them are filled in quartz fractures in irregular veins and branch states.

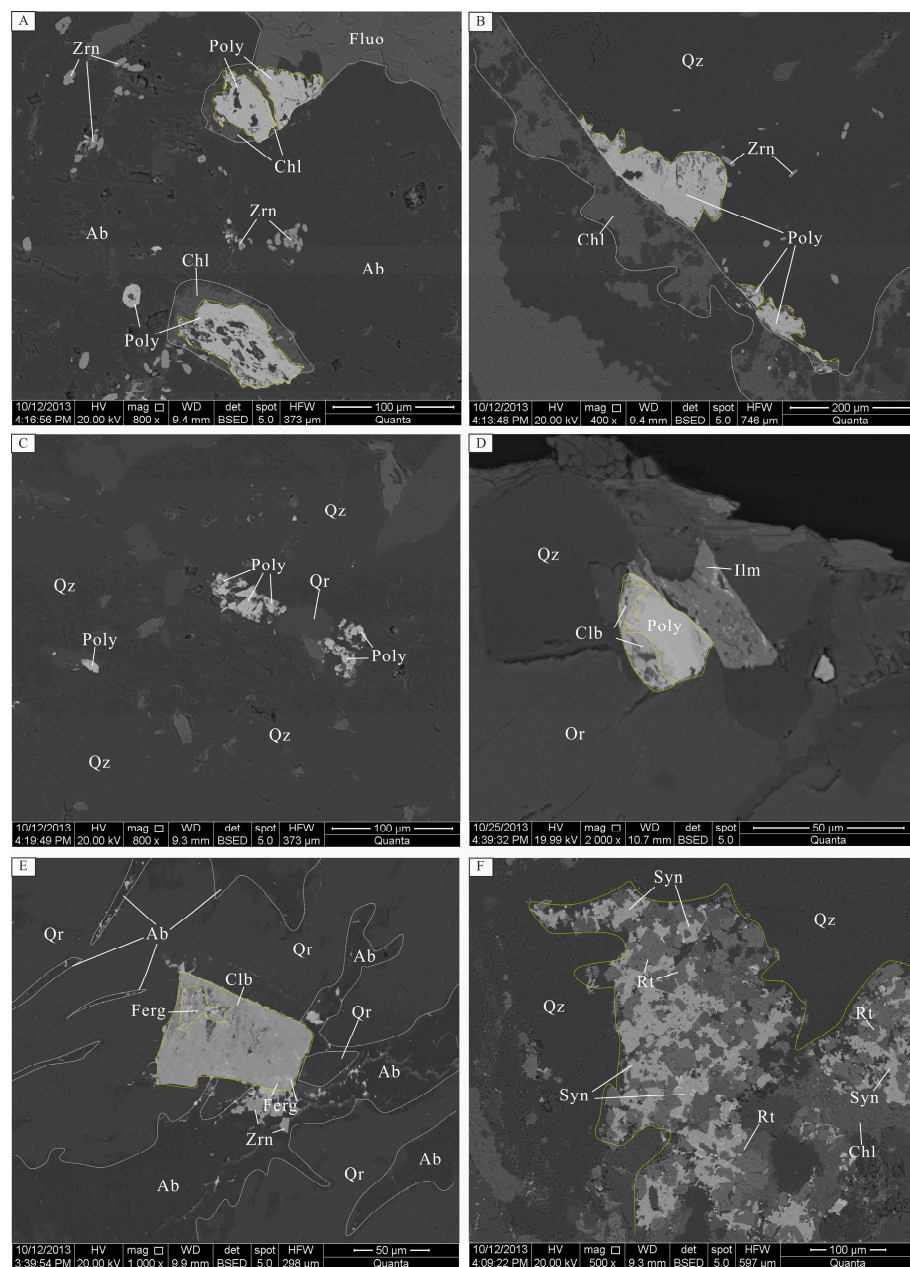


Figure 5. SEM BSE images of polycrase, columbite, and rutile in the ores (Ab, albite; Chl, chlorite; Zrn, zircon; Poly, polycrase; Fluo, fluorite; Qz, quartz; Or, orthoclase; Ferg, fergusonite; Mag, magnetite; Clb, columbite; Ilm, ilmenite; Rt, rutile; Syn, synchysite). (A) Polycrase disseminated in albite in the state of anhedral granular; chlorite distributed around the particles; dissolved pores and fissures can commonly be found inside of the particles; chlorite filled in the parts of fissures and intergrowths with fluorite. (B) Anhedral polycrase granular is embedded in quartz and growths with chlorite particle or chlorite veins; dissolved pores and fissures can be found around the particles of polycrase; polycrase crystals with slightly oriented deform and break. (C) Polycrase disseminated in the micro-fine particles of orthoclase and quartz; a small amount of chlorite exists around the polycrase, most of which is broken. (D) The polycrase intergrowths with ilmenite, and two of them are disseminated in the quartz and orthoclase; anhedral granular columbite re-works the outside of polycrase particles. (E) Columbite is disseminated in the orthoclase and contains a small amount of fergusonite. Columbite connects with irregular albite fine veins, which are generally filled in feldspar cracks; anhedral granular fergusonite and zircon occur in the fine veinlets. (F) Irregular aggregates of micro-fine rutile, synchysite, and chlorite in quartz fractures.

The content of polycrase in the ore is 0.0231 wt.%, which is slightly less than that of fergusonite. The polycrase crystal is anhedral granular. It has commonly irregular dissolution cavities and fissures filled by metamorphic minerals such as quartz, albite, chlorite, etc., with grain sizes of 5–160 μm . The disseminated types can be seen in the ore rocks (Figure 5A–D): (1) anhedral crystal of polycrase commonly associated with chlorite and disseminated into orthoclase and quartz (Figure 5A–C); (2) polycrase is associated with ilmenite, and both are disseminated into quartz and feldspar (Figure 5D). The polycrase grain size varies greatly from the coarsest, 120 μm , to fine, measuring only a few microns.

Low-content columbite in the ore rocks formed from metasomatized polycrase and fergusonite and intergrown with polycrase or fergusonite (Figure 5E). Sometimes, columbite is associated with albite. It contains a small amount of metasomatized residual of fergusonite and sometimes fills the visible fissures into the orthoclase (Figure 5E). Columbite generally contains the highly rare earth element yttrium.

The percentage of pyrochlore is only 0.0032 wt.% in the ore, which is generally disseminated into feldspar and quartz as idiomorphic crystals (Figure 6A,B). Occasionally, microfine pyrochlore grains are found in quartz crystals (Figure 6C) and magnetite crystals (Figure 6D).

The amount of aeschynite is very low. Occasionally, the anhedral granular aeschynite is an assemblage with zircon and bastnaesite and irregular veins in quartz (Figure 6E).

Microlite is the least prevalent Nb mineral in the ore, with a percentage content of 0.0024 wt.%. It embeds into orthoclase and albite crystals as a state of idiomorphic crystal. The phenomenon of filling metasomatism of the fine magnetites can be seen around the edge of mineral crystals (Figure 6F).

Ilmenorutile is associated with chlorite in the ore. Fine-grained rutile is distributed in aggregates with chlorite and other rare earth minerals in the ore (Figure 5F).

5.3. The Occurrence State and Abundance of Rare Earth Elements in Nb Minerals

Microscopic observation and EPMA energy spectrum analysis showed that the Nb-Ta ore minerals are distributed in a star-like pattern (Figures 4–6), and some of them are arranged in certain a direction (Figure 3K). Most Nb-Ta ore minerals are subhedral-anhedral granular aggregates. Some of them are connected with magnetite, ilmenite, and zircon. In addition, some of them are wrapped in quartz or feldspar. At the same time, they are also distributed in the intergranular zones and fissures of feldspar and quartz particles in a state of veins and agglomerates. The grain size of independent minerals containing Nb-Ta is in the range of 5–100 μm .

The chemical compositions of fergusonite, polycrase, columbite, Nb-rutile, ilmenorutile, aeschynite, pyrochlore, and microlite were determined by EDS (Table 3). Fergusonite generally contains uranium and thorium. Nb_2O_5 content is 38.02%–51.44% (mean, 46.80%); the Ta_2O_5 content is 0%–2.83% (mean, 1.49%); and the RE_2O_3 content is 27.42%–60.20% (mean, 42.90%). Polycrase generally contains small amounts of uranium and thorium. The Nb_2O_5 content is 27.51%–41.88% (mean, 33.24%); Ta_2O_5 content is 0.67%–5.66% (mean, 2.16%); and RE_2O_3 content is 16.14%–33.13% (mean, 23.54%). Columbite is Nb-rich and Ta-poor, generally containing Y and individually containing Ce and small amounts of silicon, calcium, titanium, uranium, and thorium. The content of Nb_2O_5 is 38.02%–51.44% (mean, 62.35%); Ta_2O_5 is 0%–2.83% (mean, 3.28%); RE_2O_3 is 1.59%–7.22% (mean, 3.36%); FeO is 5.46%–20.90% (mean, 16.00%); and MnO is 1.60%–13.38% (mean, 4.17%). Aeschynite is rich in Nb, light rare earth elements, and Th. The Nb_2O_5 content is 27.44%–38.71% (mean, 31.71%); Ta_2O_5 content is 0.33%–7.99% (mean, 3.54%); and RE_2O_3 content is 18.19%–41.74% (mean, 28.39%). Pyrochlore is enriched with Y and contains a high content of U. The Nb_2O_5 content is 54.17%–72.87% (mean, 62.94%); Ta_2O_5 content is 0.65%–5.25% (mean, 3.17%); and RE_2O_3 content is 1.95%–10.09% (mean, 5.45%). The content of Nb_2O_5 in rutile is 0.38%–2.88%, and the content of Nb_2O_5 in ilmenorutile is 5.10%–26.52%.

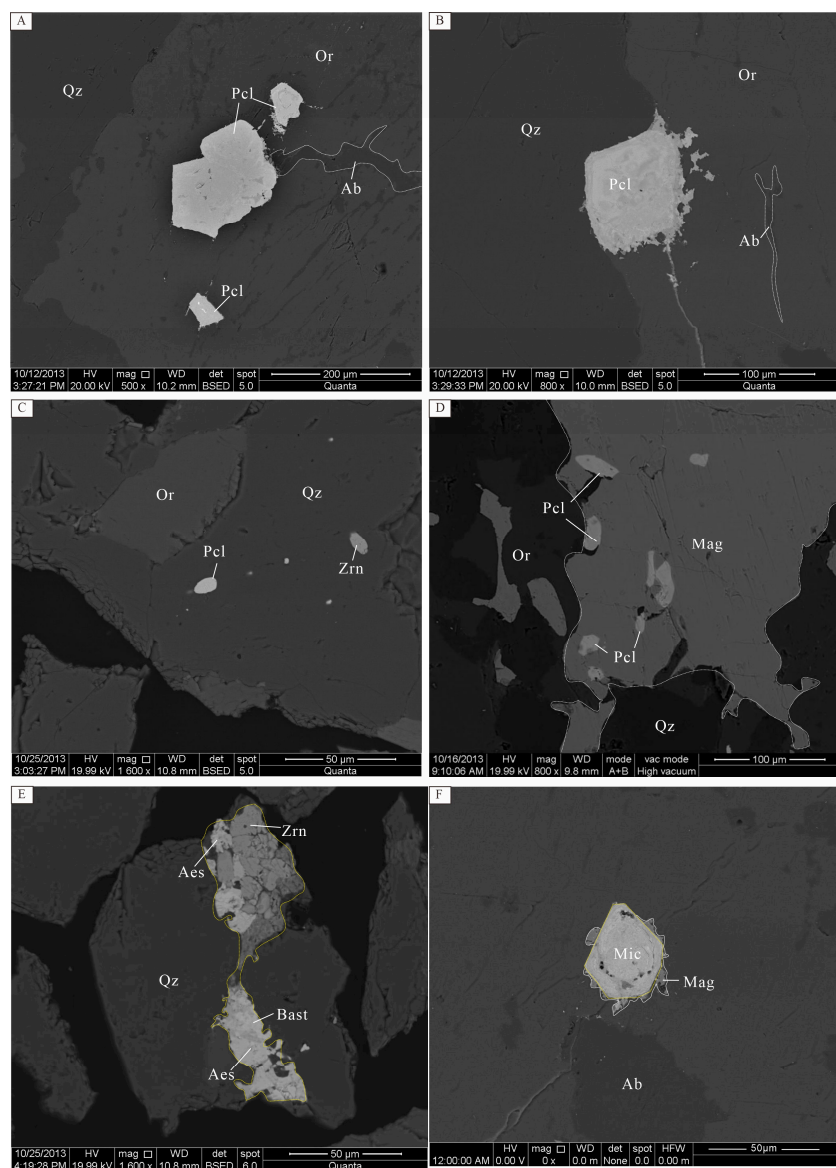


Figure 6. SEM BSE images of pyrochlore, aeschynite and microcrite in ores (Ab, albite; Qz, quartz; Or, orthoclase; Pcl, pyrochlore; Zrn, zircon; Mag, magnetite; Aes, aeschynite; Bast, bastnasite; Mic, microcrite). (A) The euhedral crystal of pyrochlore is disseminated in orthoclase and is partially associated with irregular albite fine veins. (B) Euhedral pyrochlore disseminated in orthoclase and quartz; orthoclase is seen in the albite fine veins. (C) Euhedral pyrochlore disseminated in orthoclase and albite. (D) Micro-fine euhedral-subhedral pyrochlore forms in magnetite; magnetite and secondary quartz connect and fill in the fractures of orthoclase the state of irregular veins. (E) The aggregates of anhedral granular aeschynite, subhedral-anhedral granular zircon, and anhedral granular bastnasite fill in the quartz fractures in the state of veins. (F) Euhedral crystal microcrite disseminated in orthoclase; micro-fine anhedral granular magnetite fills and replaces around the outside of microcites.

Table 3. The element percentage content results of the electron probing and EDS analysis for the main Nb minerals.

Main Nb Minerals	Fergusonite	Polyrace	Columbite	Nb-Rutile	Ilmenorutile	Aeschynite	Pyrochlore	Microlite
Empirical formula	YNbO ₄	Y(Nb, Ti) ₂ O ₆	(Fe, Mn)(Nb, Ta) ₂ O ₆	TiO ₂	(Ti, Nb, Ta, Fe)O ₂	(Ce, Y, Th, Na, Ca, Fe ²⁺)(Ti, Nb, Fe ³⁺) ₂ O ₆	(Ca, Na) ₂ Nb ₂ O ₆ (OH, F)	(Ca, Na) ₂ (Ta, Nb) ₂ O ₆ (O, OH, F)
Number of measurement points	10	8	15	5	5	13	10	3
Nb ₂ O ₅	Range	38.02–51.44	27.51–41.88	45.85–73.27	0.38–2.88	5.1–26.52	27.44–38.71	54.17–72.87
	Average	46.80	33.24	62.35	1.84	17.63	31.71	62.94
Ta ₂ O ₅	Range	0–2.83	0.67–5.66	0.67–7.31	0	0	0.33–7.99	0.65–5.25
	Average	1.49	2.16	3.28	0	0	3.54	3.17
Y ₂ O ₃	Range	19.34–30.98	11.86–15.10	1.59–6.57	0	0	3.57–7.21	1.84–5.87
	Average	26.91	13.59	3.28	0	0	4.95	4.01
Nd ₂ O ₃	Range	0.06–2.55	0–3.67	0	0	0	7.18–10.25	0.11–2.32
	Average	1.28	1.55	0	0	0	8.05	0.8
Dy ₂ O ₃	Range	3.74–6.1	1.87–3.80	0	0	0	0–1.84	0
	Average	4.82	2.73	0	0	0	0.97	0
Er ₂ O ₃	Range	1.74–4.21	0.72–2.45	0	0	0	0–0.07	0
	Average	2.69	1.2	0	0	0	0.01	0
Gd ₂ O ₃	Range	1.22–4.4	0.88–2.15	0	0	0	0–1.47	0
	Average	2.5	1.56	0	0	0	0.56	0
Yb ₂ O ₃	Range	1.32–4.39	0.66–2.23	0	0	0	0–0.2	0
	Average	2.7	1.15	0	0	0	0.06	0
Ce ₂ O ₃	Range	0–3.6	0–2.12	0–0.57	0	0	5.63–14.84	0–1.41
	Average	0.67	0.82	0.08	0	0	10.1	0.43
Sm ₂ O ₃	Range	0–2.68	0.15–1.61	0	0	0	0	0
	Average	1.18	0.94	0	0	0	0	0
La ₂ O ₃	Range	0–1.29	0	0	0	0	1.43–4.16	0–0.49
	Average	0.15	0	0	0	0	2.75	0.22
Pr ₂ O ₃	Range	0	0	0	0	0	0.38–1.70	0
	Average	0	0	0	0	0	0.95	0
UO ₂	Range	0.24–2.9	0–2.04	0–2.87	0	0	0.38–2.82	0–7.19
	Average	1.13	1.13	0.57	0	0	0.87	0.81
ThO ₂	Range	0–8.49	0–5.18	0–1.69	0	0	2.42–7.40	0–1.39
	Average	3.25	3.39	0.66	0	0	4.64	0.32
TiO ₂	Range	0–2.77	20.74–30.43	0.45–18.45	89.47–95.66	59.80–77.53	24.49–30.23	1.74–11.26
	Average	0.62	26.69	7.66	92.78	68.48	26.35	6.94
FeO	Range	0.04–5.79	1.7–5.25	5.46–20.90	1.44–6.06	7.8–18.98	0.74–2.88	0.2–6.51
	Average	1.58	3.84	16.00	3.39	12.17	1.87	1.37
Al ₂ O ₃	Range	0.28–1.64	0–0.45	0.15–1.41	0.11–1.36	0–1.09	0	0
	Average	0.75	0.29	0.59	0.62	0.43	0	0
CaO	Range	0.28–4.26	2–4.97	0.09–1.65	0	0	1.11–5.74	11.13–22.95
	Average	1.48	2.89	0.7	0	0	2.64	17.23
MnO	Range	0	0.30–3.49	1.60–13.38	0	0	0	0.34–1.23
	Average	0	0.81	4.17	0	0	0	0.68
SiO ₂	Range	0	1.54–2.29	0–2.95	0.52–2.34	0–2.96	0	0
	Average	0	2.01	0.67	1.32	1.18	0	0
MgO	Range	0	0	0	0–0.25	0–0.56	0	0
	Average	0	0	0	0.05	0.11	0	0
Na ₂ O	Range	0	0	0	0	0	0	0–3.78
	Average	0	0	0	0	0	0	0.8–3.71
PbO	Range	0	0	0	0	0	0	0.55–11.72
	Average	0	0	0	0	0	0	4.32
F	Range	0	0	0	0	0	0	0.1–2.84
	Average	0	0	0	0	0	0	0.53–2.37

6. Discussion

6.1. Major Nb-Minerals and Occurrence State

The main Nb-bearing minerals species of the Yushishan Nb-Ta ore deposit have always been disputed for two reasons. The first reason is related to differences in analysis methods. Jia (2016) found that rutile is the main Nb-bearing and Ta-bearing mineral, and monazite

contains only small amounts of Nb based on observing the thin slices [40]. Chen et al. (2022) found that Nb minerals are mainly columbite, fergusonite, pyrochlore, and Nb-rutile by SEM and EDS [36]. The second reason is the fine grain size of Nb minerals and Nb-bearing minerals in the ore, mostly in the range of 5–80 μm (Table 2). Thus, the naked eye cannot observe Nb minerals and Nb-bearing minerals in the ores (Figure 3C–F). In addition, it is difficult to identify metal minerals such as magnetite under a micropolariscope (Figure 3G–J). Regarding SEM, a large number of measurement points are required in the identification process to obtain representative results due to the small field of view. Therefore, when using a micropolariscope and SEM to identify fine minerals, the results of mineral identification will be incomplete.

We have analyzed a large number of samples using the MLA high-precision automatic quantitative mineral analysis system. The results obtained for mineral species are relatively comprehensive (Table 1), and in particular, low-content Nb-bearing minerals are accurately determined (Table 4). SEM and EDS analysis revealed that the minerals with high Nb contents are mainly fergusonite (mean, 46.80%), columbite (mean, 62.35%), polycrase (mean, 33.24%), aeschynite (mean, 31.71%), pyrochlore (mean, 62.94%), microlite (mean, 26.36%), ilmenorutile (mean, 17.63%), and Nb-rutile (mean, 1.84%). Magnetite/magnetic hematite (mean, 0.25%), magnetic veinlets (mean, 0.06%), and non-magnetic veinlets (mean, 0.001%) contain very low levels of Nb (Figure 7, Table 4).

Table 4. Statistical analysis of the Nb occurrence state in ores and the contribution rate of each mineral to the ores.

Occurrence States	Nb-Bearing Minerals	Mineral Contents (wt.%)	Nb ₂ O ₅ Contents in Minerals (%)	Nb ₂ O ₅ Contents in Ores (%)	The Nb Contribution Rate of Minerals to Ores (%)
Nb minerals	Fergusonite	0.0248	46.8	0.0116	22.46
	Columbite	0.0126	62.35	0.0079	15.20
	Polycrase	0.0231	33.24	0.0077	14.86
	Nb-rutile	0.1817	1.84	0.0033	6.47
	Aeschynite	0.0066	31.71	0.0021	4.05
	Pyrochlore	0.0032	62.94	0.0020	3.90
	Microlite	0.0024	26.36	0.0006	1.22
Magnetic iron mineral	Ilmenorutile	0.0028	17.63	0.0005	0.96
	Titanium magnetite/maghemitite	3.745	0.247	0.0093	17.90
Gangue	Magnetic gangue	9.9945	0.0604	0.0060	11.68
	Non-magnetic gangue	85.1437	0.0008	0.0007	1.32

We also calculated the Nb₂O₅ content of each mineral in the ores and their contributions to the whole rock (Table 4). The average content of Nb₂O₅ in Nb-bearing leptynites is 0.0517% (Table 4). There are three main modes of occurrence of Nb. The first Nb minerals are 0.2572 wt.%, contributing 69.11% of Nb in the ore (Table 4). They are mainly fergusonite (0.0248 wt.%), columbite (0.0126 wt.%), polycrase (0.0231 wt.%), Nb-rutile (0.1817 wt.%), aeschynite (0.0066 wt.%), pyrochlore (0.0032 wt.%), microlite (0.0024 wt.%), and ilmenorutile (0.0028 wt.%). The second mode of occurrence of Nb-bearing minerals is as microinclusions dispersed in titanomagnetite–magnetite hematite. The total content of titanomagnetite–magnetite minerals is 3.745 wt.%, which contributes to 17.90% of Nb (Table 4). The third mode of occurrence is dispersed as micro-scale grains in magnetic and non-magnetic gangues. The content in the gangue minerals is 95.1382%, each contributing to 11.68% and 1.32% of Nb (Table 4).

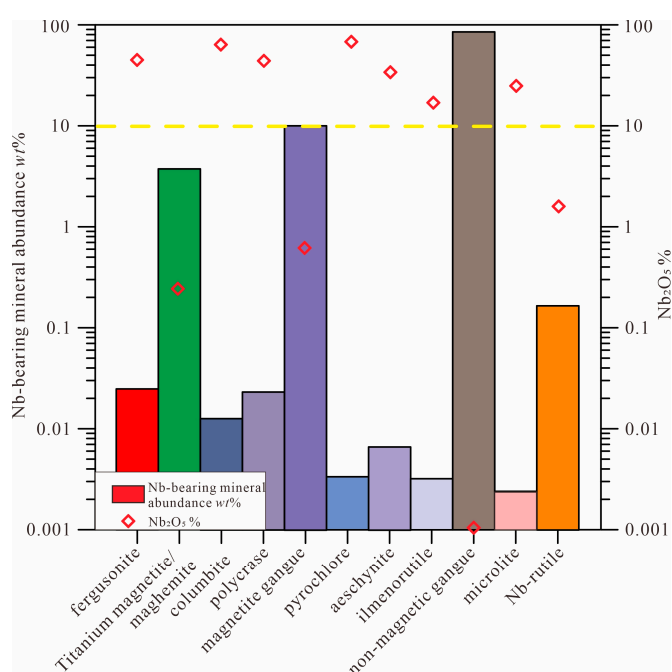


Figure 7. Nb-bearing minerals and Nb content of the Yushishan Nb–Ta ore deposit.

The results show that Nb in the Yushishan Nb–Ta ore deposit mainly occurs in fergusonite, columbite, polycrase, Nb-rutile, aeschynite, pyrochlore, microlite, and ilmenorutile, with an abundance of about 69.11% (Figure 7, Table 4). The main Nb minerals in the ores are fergusonite, columbite, and polycrase. The abundance of Nb in these three minerals is more than 14% separately (Figure 7, Table 4). Additionally, Nb-rutile, aeschynite, pyrochlore, microlite, and ilmenorutile each contributed less than 10% to the ores, and the total Nb contributing to the ores is 16.59%. The total Nb contributing to the ores in Nb-rutile and ilmenorutile is only 7.43% (Figure 7, Table 4).

6.2. Mineralogical Mechanism and Nb–Ta Two-Stage Mineralization Model

Since the discovery of the Yushishan Nb–Ta ore deposit in 2011, its mineral occurrence has been investigated by several researchers [36,37,40,51]. These researchers have mainly focused on researching the ages of diagenesis, mineralization, and geochemical characteristics of leptynite. Jia (2016) found that the ore-forming protolith was formed at approximately 829.4 Ma and was affected by metamorphism at approximately 790 Ma based on the zircon U–Pb dating of hosting leptynite [40]. Chen et al. (2022) determined that the U–Pb ages of magmatic zircons in the hosting leptynite are 791–833 Ma, and the protolith formation age is at 812–814 Ma [36]. They observed that the main Nb–Ta mineralization period occurred in the Neoproterozoic Era during the breaking of the Rodinia supercontinent. Many metamorphic zircons with U–Pb ages of 472–770 Ma were also found, representing multi-stage metamorphism in this area [36]. Liu et al. (2022) provided two thermal events in the Yushishan area according to zircon U–Pb and titanite dating [43]. The first stage occurred at 834–790 Ma (zircon U–Pb age), and the second stage occurred at 490–470 Ma (titanite and zircon). The latter is the main metallogenic period of Nb–Ta ore. Jiang et al. (2022) measured zircon U–Pb ages in leptynites, which in ore-free leptynites were mainly 831 ± 5 Ma– 790 ± 5 Ma, and which in hosting leptynites were at 491 ± 4 Ma to 455 ± 4 Ma [37]. They hypothesized that 490–455 Ma was the main Nb–Ta metallogenic period [37].

Based on the regional tectonic evolution [52–55] and geochemical characteristics of the Nb–Ta ore deposit, we hold the view that the formation ages (834–790 Ma) of magmatic zircon in leptynite represent the formation ages of protolith, corresponding to the breaking of Rodinia. The metamorphic zircon ages of leptynite are 455–770 Ma, and the peak ranges

were primarily concentrated in 455–490 Ma. This was the period in which the Northern Altun Tagh Block was subducted to the western part of the Central Qilian Block to the west. However, the main Nb-Ta mineralizing period is now an open question; one view is that Nb-Ta mineralization mainly occurs in the magmatism process of leptynite protoliths (834–790 Ma) [36,40], and another view is that Nb-Ta mineralization mainly forms in the hydrothermal metamorphic process at 455–490 Ma [37,43].

The zircon has an evident hydrothermal alteration phenomenon and grow with Nb minerals based on the SEM observations (Figure 4A–D,E,F). This indicates that the magmatic genesis and hydrothermal genesis of Nb minerals occurred. Later, hydrothermal activities modified part of euhedral fergusonite, polycrase, pyrochlore, and microlite. These are found in the crystals of quartz, feldspar, and magnetite or in the mineral interstitials of leptynite (Figure 4A–D, Figures 5D and 6A,B). Nb-bearing minerals may form from magma [56–58]. The Yushishan Nb-Ta ore deposit formed in the magmatic activity at 834–790 Ma and was then transformed by hydrothermal activity, migration, and enrichment into a Nb ore deposit during 490–455 Ma. Chloritization, albitization, and silicification in the Nb-Ta ore deposit have been observed in field stratigraphic sections. It has been observed under SEM that some Nb minerals are reworked and are closely associated with secondary metamorphic minerals (Figure 5A–D and Figure 6D,F). Polycrase develops internal fractures and multiple suspected dissolution pores (Figure 5A–D and Figure 6D,F). At the same time, the fractures are filled with metamorphic minerals such as chlorite, albite, and secondary quartz (Figure 5A–D and Figure 6D,F). This indicates that polycrase has been hydrothermally reworked and rare metal elements such as Nb and Ta have migrated out. There is metasomatism between niobium minerals. The fine granular columbite is produced around the edge of the crystal of the polycrase and replaces the polycrase (Figure 5D). Moreover, the phenomena of columbite wrapping and replacing fergusonite can also be seen (Figure 5E). These characteristics indicate that the hydrothermal metasomatism replaced Nb minerals formed in the early stage of the ore to form new Nb-bearing minerals, such as columbite, anhedral fergusonite, aeschynite, and Nb-rutile.

In summary, Nb minerals can be divided into two types according to the mineralization stage. The first type is magmatic mineralization. Euhedral–subhedral granular Nb minerals occur as inclusions in, or in interstitial positions among, quartz, feldspar, and other minerals, suggesting that minerals are formed simultaneously with these igneous minerals. The main Nb minerals formed are fergusonite, polycrase, pyrochlore, and microlite. The second type is hydrothermal mineralization. Different Nb minerals occur in ore fissures in a state of irregular veins and agglomerated aggregates. These Nb minerals are closely associated with metamorphic minerals such as chlorite, albite, and secondary quartz. The direct metasomatic origin among different Nb minerals can be seen locally, including columbite, fergusonite (anhedral granular), Nb-rutile, and aeschynite. Due to the host-rocks of the magmatic mineralization stage being affected by regional tectonic–thermal events, rare metal elements such as Nb were mobilized by later hydrothermal fluids and enriched Nb-Ta ore in the favorable host rock, such as mineral fissures, gaps, and edges of primary Nb minerals.

6.3. Metallogenetic Model of the Leptynite Nb-Ta Ore Deposit in the Western Part of Central Qilian Orogenic Belt

Mineral compositions and microscopic crystal structures of the Yushishan Nb-Ta ore deposit have been determined. Furthermore, we combine the archives of the recovery and formation background of the leptynite protoliths [36,37,40,43]. Mineralization at the Yushishan leptynite-type Nb-Ta ore deposit is divided into the following stages (Figure 8).

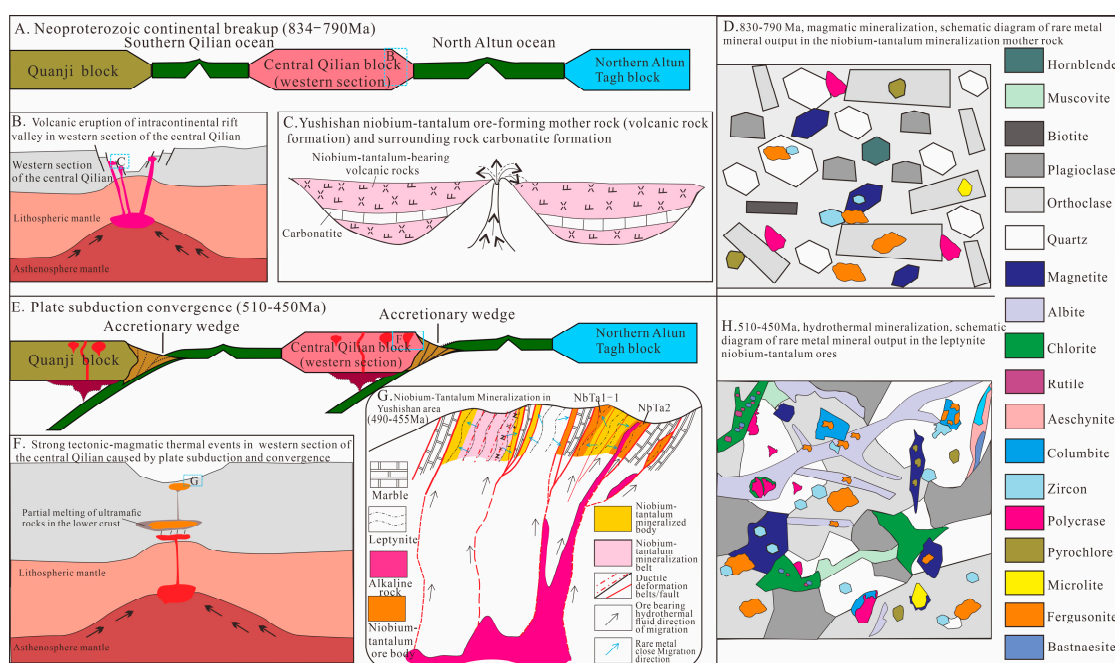


Figure 8. Comprehensive metallogenic model of leptynite-type Nb-Ta ore deposit in the western part of the Central Qilian. (B,F) adapted from Jiang et al. (2022) [37]; (A–D), the first stage of Nb-Ta mineralization in the western part of Central Qilian at 834–790 Ma; (E,F) the second stage of Nb-Ta mineralization at 490–455 Ma; (G,H) share the right-column’s legend.

(1) The block of the western part of Central Qilian rifted during the Neoproterozoic Era (834–790 Ma). The Nb-rich intermediate-felsic magmatic rocks were formed in the Yushishan.

The Northwestern China paleo-continent responded to subsequent rifting events (850–700 Ma) [55,59,60] after the convergence of the Rodinia supercontinent (1000–900 Ma) [51]. The tectonic location of the study area is in the western part of the Central Qilian Block. The north of the study area is adjacent to the eastern part of the Altun Tagh Block, and the south is adjacent to the northern part of the northern margin of the Qaidam Block (Figure 1). These three tectonic units were in the process of continental rifting during the middle and late Neoproterozoic Era (834–790 Ma) (Figure 8A), corresponding to the rifting stage of the Rodinia supercontinent [53,55,61–66]. The protolith of the hosting leptynite of the Yushishan Nb-Ta ore deposit was formed in the middle–late Neoproterozoic Era. Its petrogenetic age is 834–790 Ma [36,37,43], which corresponds to the tectonic setting of continental rifting in the region. Chen et al. (2022) showed that the protoliths of leptynite were intermediate-felsic magmatic rocks that erupted in an intracontinental rift environment [36,37]. The upwelling of the lithosphere and asthenosphere triggered intracontinental rifting and led to volcanic eruption (Figure 8B). Thus, the intermediate-felsic Nb-Ta ore-forming protolith rich in rare metal elements such as Nb were formed and intruded into the carbonatite wall rocks (Figure 8C). In the ore-forming protolith, Nb minerals such as fergusonite, polycrase, pyrochlore, microlite, and rare metal minerals such as zircon are formed (Figure 8D). The initial enrichment of Nb, Ta, and other rare metals occurred during this stage in the Yushishan deposit.

(2) The Quanji Block in the northern boundary of Qaidam Basin, the western part of the Central Qilian Block, and the northern boundary of Altun Tagh Block subducted and converged during the Caledonian period (510–450 Ma). This caused strong tectonic-magmatic thermal events, which led to the activation and enrichment of Nb and other rare metals in the ore host-rocks in the western part of the Central Qilian. This was the second stage of Nb-Ta mineralization.

The Quanji Block in the northern boundary of Qaidam Basin and the western part of the Central Qilian Block, as well as the northern boundary of Altun Tagh Block, is located in the plate convergence and subduction tectonic environment at 510–450 Ma [52–54,64,67–70]. During this period, the Northern Altun Tagh ocean and the Southern Qilian ocean subducted southward [52,64]. Liao et al. (2020) suggested that monzogranite in the Yushishan Nb-Ta ore deposit was closely associated with the formation of the South Qilian continental crust with the southward subduction of the North Altun Tagh oceanic crust in the early Ordovician (481.3 ± 1.7 Ma) [42]. The U–Pb ages of metamorphic zircons in the Yushishan leptynite-type Nb-Ta ore deposit are mainly within 490–455 Ma [37,39,40,43]. This is consistent with the formation ages of the North Qilian–North Altun Tagh HP/LT metamorphic belts [71].

During the Caledonian period (510–450 Ma), the Northern Altun Tagh Block subducted from north to south due to the convergence and subduction of regional plates (Figure 8E). It induced upwelling of the lithosphere and asthenosphere in the western part of Central Qilian [72]. A series of long-lasting, extensive, and intense tectonic–magmatic thermal events occurred (Figure 8F). During 490–455 Ma, the intermediate-felsic magmatic rocks and carbonatite were metamorphosed to leptynite and marble in the Yushishan area, respectively. Hydrothermal alteration phenomena such as chloritization, albitization, silification, and potassium alteration occurred in the leptynite. The hydrothermal alterations activated rare metal elements such as Nb in the ore-forming host rocks (niobium-rich magmatic rocks). Eventually, Nb-Ta ore bodies formed in the favorable host rocks (Figure 8G). However, there was no Nb mineralization in the roof and base plate marbles. Thus, we can find a large number of hydrothermal mineralization phenomena and hydrothermal Nb minerals in leptynite-type Nb-Ta ore deposits, such as columbite, anhedral fergusonite, aeschynite, Nb-rutile, and bastnaesite. At the same time, the modified primary Nb minerals such as polycrase, euhedral–subhedral fergusonite, pyrochlore, and microlite are retained (Figure 8H).

(3) Contribution of two types of mineralization processes to the mineralization of leptynite-type Nb-Ta ore deposit at two stages.

Jia (2016) and Chen et al. (2022) emphasized that Neoproterozoic magmatism was a significant leptynite type Nb-Ta mineralization in the western part of the Central Qilian Mountains [36,40]. Jiang et al. (2022) believed that the hydrothermal process between 491 ± 4 Ma and 455 ± 4 Ma was the main metallogenic stage [37]. We found that magmatic Nb-bearing minerals (fergusonite, polycrase, pyrochlore, and microlite) in Yushishan leptynite contributed approximately 19.98%–42.43% Nb to the Nb-Ta ore deposits, without excluding the hydrothermal fergusonite proportion. Hydrothermal Nb-bearing minerals (columbite, fergusonite, aeschynite, and Nb-rutile) contributed approximately 26.67%–49.13% Nb to the Nb-Ta ore deposit, including magmatic fergusonite. The contribution of Neoproterozoic (834–790 Ma) magmatism and Caledonian (490–455 Ma) hydrothermal effect to leptynite-type Nb-Ta ore deposits is approximately the same. Therefore, the leptynite-type Nb-Ta ore deposit in the study area is a mixed type of Nb-Ta ore deposit.

7. Conclusions

There are three modes of occurrence of Nb in the Yushishan Nb-Ta ore deposit: (1) Nb occurs in minerals such as fergusonite, columbite, polycrase, and Nb-rutile, accounting for 69.11% of the total Nb in the ore; (2) microscopic inclusions of Nb minerals dispersed in titanomagnetite–magnetite hematite, which account for 17.90% of the total Nb in the ore; (3) microscopic inclusions of Nb minerals dispersed in gangue, accounting for 13.00% of the total Nb in the ore.

The main Nb minerals in the Yushishan Nb-Ta ore deposit are fergusonite, columbite, and polycrase. They contribute 52.51% Nb to the ore. Among them, Nb is mostly hosted in fergusonite, reaching 22.46% Nb. The total Nb percentage of Nb-rutile, aeschynite, pyrochlore, microlite, and ilmenorutile is less than 10%. These minerals contribute 16.59% Nb to the ore.

Nb minerals in leptynite ores have two genetic types, which are formed in two stages impacted by tectonic activities. The first stage (834–790 Ma) is magmatic. Nb minerals are euhedral–subhedral particles distributed in quartz, feldspar, and other primary mineral crystals or crystal gaps. Nb minerals are formed together with the primary minerals, including euhedral–subhedral fergusonite, polycrase, pyrochlore, and microlite. The second stage (510–450 Ma) is hydrothermal. Different Nb minerals in a state of irregular veins and agglomerated aggregates filled in the ore and primary mineral fissures. They are closely associated with metamorphic minerals such as chlorite, albite, and secondary quartz. At the same time, direct metasomatism among different Nb minerals can be seen locally, including columbite, anhedral granular fergusonite, Nb-rutile, and aeschynite. The two mineralization stages contributed roughly equal Nb to the Yushishan Nb–Ta ore deposit.

Author Contributions: Conceptualization, J.Y.; Data curation, J.Y.; Formal analysis, Y.W. and C.Z. (Chunhui Zhang); Investigation, H.S. and D.S.; Methodology, J.Y. and Y.W.; Supervision, C.Z. (Chengjun Zhang); Writing—original draft, J.Y. and Y.W.; Writing—Review and editing, C.Z. (Chunhui Zhang) and C.Z. (Chengjun Zhang). All authors have read and agreed to the published version of the manuscript.

Funding: This work was financially supported by projects from the Ministry of Science and Technology (MOST) National Key R&D Program of China (No. 2017YFC0602400), Geological Exploration Fund Project of Gansu Province, China.

Data Availability Statement: Not applicable.

Acknowledgments: We would like to thank the editor and anonymous reviewers for their constructive comments. We would like to thank Shaoyong Jiang, Xiaofeng Cao, and Wei Chen for their constructive suggestions in fieldwork.

Conflicts of Interest: The authors declare no conflict of interest.

References

1. Mackay, D.A.R.; Simandl, G.J. Geology, market and supply chain of niobium and tantalum—A review. *Miner. Depos.* **2014**, *49*, 1025–1104. [[CrossRef](#)]
2. Melcher, F.; Graupner, T.; Gäbler, H.E.; Sitnikova, M.; Henjes-Kunst, F.; Oberthür, T.; Gerdes, A.; Dewaele, S. Tantalum–(niobium–tin) mineralisation in African pegmatites and rare metal granites: Constraints from Ta–Nb oxide mineralogy, geochemistry and U–Pb geochronology. *Ore Geol. Rev.* **2015**, *64*, 667–719. [[CrossRef](#)]
3. Dostal, J.; Gerel, O. Occurrences of Niobium and Tantalum Mineralization in Mongolia. *Minerals* **2022**, *12*, 1529. [[CrossRef](#)]
4. Li, J.K.; Li, P.; Wang, D.H.; Li, X. A review of niobium and tantalum metallogenetic regularity in China. *Chin. Sci. Bull.* **2019**, *64*, 1545–1566, (In Chinese with English Abstract). [[CrossRef](#)]
5. Dill, H.G. The “chessboard” classification scheme of mineral deposits: Mineralogy and geology from aluminum to zirconium. *Earth Sci. Rev.* **2010**, *100*, 1–420. [[CrossRef](#)]
6. Kendall-Langley, L.A.; Kemp, A.I.; Grigson, J.L.; Hammerli, J. U–Pb and reconnaissance Lu–Hf isotope analysis of cassiterite and columbite group minerals from Archean Li–Cs–Ta type pegmatites of Western Australia. *Lithos* **2020**, *352*, 105231. [[CrossRef](#)]
7. Jiang, S.; Su, H.; Xiong, Y.; Liu, T.; Zhu, K.; Zhang, L. Spatial-Temporal Distribution, Geological Characteristics and Ore-Formation Controlling Factors of Major Types of Rare Metal Mineral Deposits in China. *Acta Geol. Sin. Engl. Ed.* **2020**, *94*, 1757–1773. [[CrossRef](#)]
8. Xiong, Y.-Q.; Jiang, S.-Y.; Wen, C.-H.; Yu, H.-Y. Granite–pegmatite connection and mineralization age of the giant Renli TaNb deposit in South China: Constraints from U–Th–Pb geochronology of coltan, monazite, and zircon. *Lithos* **2020**, *358*, 105422. [[CrossRef](#)]
9. Van Lichtervelde, M.; Salvi, S.; Beziat, D.; Linnen, R.L. Textural features and chemical evolution in tantalum oxides: Magmatic versus hydrothermal origins for Ta mineralization in the Tanco Lower Pegmatite, Manitoba, Canada. *Econ. Geol.* **2007**, *102*, 257–276. [[CrossRef](#)]
10. Belkasmi, M.; Cuney, M.; Pollard, P.J.; Bastoul, A. Chemistry of the Ta–Nb–Sn–W oxide minerals from the Yichun rare metal granite (SE China): Genetic implications and comparison with Moroccan and French Hercynian examples. *Miner. Mag.* **2000**, *64*, 507–523. [[CrossRef](#)]
11. Yin, L.; Pollard, P.J.; Shouxi, H.; Taylor, R.G. Geologic and geochemical characteristics of the Yichun Ta–Nb–Li deposit, Jiangxi Province, South China. *Econ. Geol.* **1995**, *90*, 577–585. [[CrossRef](#)]
12. Li, S.; Li, J.; Chou, I.-M.; Jiang, L.; Ding, X. The formation of the Yichun Ta–Nb deposit, South China, through fractional crystallization of magma indicated by fluid and silicate melt inclusions. *J. Asian Earth Sci.* **2017**, *137*, 180–193. [[CrossRef](#)]

13. Huang, W.; Wu, J.; Liang, H.; Zhang, J.; Ren, L.; Chen, X. Ages and genesis of W-Sn and Ta-Nb-Sn-W mineralization associated with the Limu granite complex, Guangxi, China. *Lithos* **2020**, *352*, 105321. [[CrossRef](#)]
14. Wu, M.; Samson, I.M.; Zhang, D. Textural features and chemical evolution in Ta-Nb oxides: Implications for deuterian rare-metal mineralization in the Yichun granite-marginal pegmatite, southeastern China. *Econ. Geol.* **2018**, *113*, 937–960. [[CrossRef](#)]
15. Wu, M.; Samson, I.M.; Qiu, K.; Zhang, D. Concentration Mechanisms of Rare Earth Element-Nb-Zr-Be Mineralization in the Baerzhe Deposit, Northeast China: Insights from Textural and Chemical Features of Amphibole and Rare Metal Minerals. *Econ. Geol.* **2021**, *116*, 651–679. [[CrossRef](#)]
16. Wu, B.; Wen, H.-J.; Bonnetti, C.; Wang, R.-C.; Yang, J.-H.; Wu, F.-Y. Rinkite-(Ce) in the nepheline syenite pegmatite from the Saima alkaline complex, northeastern China: Its occurrence, alteration, and implications for REE mineralization. *Can. Miner.* **2019**, *57*, 903–924. [[CrossRef](#)]
17. Su, H.-M.; Jiang, S.-Y.; Zhu, X.-Y.; Duan, Z.-P.; Huang, X.-K.; Zou, T. Magmatic-hydrothermal processes and controls on rare-metal enrichment of the Baerzhe peralkaline granitic pluton, inner Mongolia, northeastern China. *Ore Geol. Rev.* **2021**, *131*, 103984. [[CrossRef](#)]
18. Salvi, S.; Williams-Jones, A.E. Alkaline granite-syenite hosted deposits. *Geol. Assoc. Can. Short Course Notes* **2005**, *17*, 315–341.
19. Liu, S.; Ding, L.; Fan, H.-R.; Yang, K.-F.; Tang, Y.-W.; She, H.-D.; Hao, M.-Z. Hydrothermal genesis of Nb mineralization in the giant Bayan Obo REE-Nb-Fe deposit (China): Implicated by petrography and geochemistry of Nb-bearing minerals. *Precambrian Res.* **2020**, *348*, 105864. [[CrossRef](#)]
20. Xu, C.; Kynicky, J.; Chakhmouradian, A.R.; Li, X.; Song, W. A case example of the importance of multi-analytical approach in deciphering carbonatite petrogenesis in South Qinling orogen: Miaoya rare-metal deposit, central China. *Lithos* **2015**, *227*, 107–121. [[CrossRef](#)]
21. Ying, Y.; Chen, W.; Lu, J.; Jiang, S.-Y.; Yang, Y. In situ U-Th-Pb ages of the Miaoya carbonatite complex in the South Qinling orogenic belt, central China. *Lithos* **2017**, *290–291*, 159–171. [[CrossRef](#)]
22. Ying, Y.-C.; Chen, W.; Chakhmouradian, A.R.; Zhao, K.-D.; Jiang, S.-Y. Textural and compositional evolution of niobium minerals in the Miaoya carbonatite-hosted REE-Nb deposit from the South Qinling Orogen of central China. *Miner. Depos.* **2023**, *58*, 197–220. [[CrossRef](#)]
23. Wang, F.L.; Zhao, T.P.; Chen, W. Advances in study of Nb-Ta ore deposits in Panxi area and tentative discussion on genesis of these ore deposits. *Miner. Depos.* **2012**, *31*, 293–308, (In Chinese with English Abstract). [[CrossRef](#)]
24. Cuney, M.; Marignac, C.; Weisbrod, A. The Beauvoir topaz-lepidolite albite granite (Massif Central, France); the disseminated magmatic Sn-Li-Ta-Nb-Be mineralization. *Econ. Geol.* **1992**, *87*, 1766–1794. [[CrossRef](#)]
25. Hildreth, W.; Chapin, C.E.; Elston, W.E. The Bishop Tuff: Evidence for the origin of compositional zonation in silicic magma chambers Tagh. *Geol. Soc. Am. Spec. Pap.* **1979**, *180*, 43–75. [[CrossRef](#)]
26. Kovalenko, V.I.; Tsaryeva, G.M.; Goreglyad, A.V.; Yarmolyuk, V.V.; Troitsky, V.A.; Hervig, R.L.; Farmer, G.L. The peralkaline granite-related Khaldzan-Buregtey rare metal (Zr, Nb, REE) deposit, western Mongolia. *Econ. Geol.* **1995**, *90*, 530–547. [[CrossRef](#)]
27. Pollard, P.J. Geochemistry of granites associated with tantalum and niobium mineralization. In *Lanthanides, Tantalum and Niobium*; Springer: Berlin/Heidelberg, Germany, 1989; pp. 145–168. [[CrossRef](#)]
28. Raimbault, L.; Cuney, M.; Azencott, C.; Duthou, J.-L.; Joron, J.L. Geochemical evidence for a multistage magmatic genesis of Ta-Sn-Li mineralization in the granite at Beauvoir, French Massif Central. *Econ. Geol.* **1995**, *90*, 548–576. [[CrossRef](#)]
29. Zhu, J.-C.; Li, R.-K.; Li, F.-C.; Xiong, X.-L.; Zhou, F.-Y.; Huang, X.-L. Topaz-albite granites and rare-metal mineralization in the Limu district, Guangxi Province, southeast China. *Miner. Depos.* **2001**, *36*, 393–405. [[CrossRef](#)]
30. Beus, A.A.; Severov, E.A.; Sitnin, A.A.; Subbotin, K.D. *Albitized and Greisenized Granites (Apogranites)*; Izdat Akad Nauk SSSR: Moscow, Russia, 1962.
31. Kempe, U.; Götze, J.; Dandar, S.; Habermann, D. Magmatic and metasomatic processes during formation of the Nb-Zr-REE deposits Khaldzan Buregte and Tsakhir (Mongolian Altai): Indications from a combined CL-SEM study. *Miner. Mag.* **1999**, *63*, 165–177. [[CrossRef](#)]
32. Salvi, S.; Williams-Jones, A.E. The role of Hydrothermal processes in concentrating HFSE in the Strange Lake peralkaline complex, northeastern Canada. *Geochim. Cosmochim. Acta* **1996**, *60*, 1917–1932.
33. Zhao, Z.H.; Zeng, T.Z.; Shabani, M.B. Quaternary grouping effect of rare earth elements on rare metal granites. *Geochimica* **1992**, *3*, 221–233, (In Chinese with English Abstract). [[CrossRef](#)]
34. Zhang, A.C.; Wang, R.C.; Hu, H.; Zhang, H.; Zhu, J.C.; Xie, L. The Complex Zonation of Niobite-group Minerals from the Koktokay No.3 Granitic Pegmatite Dyke, Altay, NW China and Its Petrological Implications. *Acta Geol. Sin.* **2004**, *78*, 181–189, (In Chinese with English Abstract). [[CrossRef](#)]
35. Yu, J.P.; Zhang, X.H.; Zhao, J.G.; Li, T.G.; Ye, D.J.; Liu, J.H. Discovery and significance of Niobium tantalum rare metal deposit in Yushishan, Altun Mountain, Gansu Province. *Miner. Depos.* **2012**, *31*, 391–392, (In Chinese with English Abstract). [[CrossRef](#)]
36. Chen, W.; Cao, X.F.; Lv, X.B.; Yang, W.; Lu, Y.Y.; Li, T.G.; Wu, Y.B. Diagenetic age and tectonic setting of Niobium-tantalum mineralized granulated protolites in Yushishan, Gansu Province. *Geotecton. Metallog.* **2022**, *46*, 755–772, (In Chinese with English Abstract). [[CrossRef](#)]
37. Jiang, S.; Liu, T.; Zhang, H.; Cao, S.; Zheng, R.; Li, T.; Yu, J.; Wu, Y. A new type of rare metal deposit: The Yushishan leptynite-type Nb-Ta deposit in eastern Altun Tagh, Gansu Province, NW China. *Acta Geol. (Engl. Ed.)* **2022**, *96*, 1471–1483. [[CrossRef](#)]

38. Yu, J.P.; Wu, Y.B.; Liang, M.H.; Xiao, P.X.; Dou, X.Y. New progress of geological mapping in the southern margin of Altyn and its implications for ore prospecting: Based on six regions of 1:50,000 Moba, Gansu. *Geol. Surv. China* **2015**, *2*, 40–47, (In Chinese with English Abstract). [[CrossRef](#)]
39. Yang, Z.Z.; Xiao, P.X.; Gao, X.F.; Kang, L.; Xie, C.R.; Yu, J.P. LA-ICP-MS Dating of the Aegirine-Augite Syenite of Yushishan Nb-Ta Deposit in Eastern Altun and Its Constraints on the Metallogenetic Age. *Northwestern Geol.* **2014**, *47*, 187–197, (In Chinese with English Abstract). [[CrossRef](#)]
40. Jia, Z.L. *Geochemical and Metallogenetical Characteristics of NB-TA-RB Deposits, South Qilian-Beishan Area, Gansu Province, China*; Lanzhou University: Lanzhou, China, 2016; (In Chinese with English Abstract).
41. Li, G.T.; Liang, M.H.; Yu, J.P.; Huang, Z.B.; Zhang, X.; Zhu, Y.X. *Metallogenetic Characteristics and Metallogenetic Regularity of Rare Metals in Gansu Province*; Geological Publishing House: Beijing, China, 2018; pp. 30–48. (In Chinese)
42. Liao, F.Y.; Chen, W.; Cao, X.F.; Chen, G.; He, K.; Yang, W.; Wu, Y.; Li, T. Petrogenesis and Forming Environment of Monzonitic Granite in Yushishan Nb-Ta Mining Area, Akesai, Gansu Province: Evidences from Chronology and Geochemistry. *Earth Sci.* **2020**, *45*, 4589–4603, (In Chinese with English Abstract). [[CrossRef](#)]
43. Liu, T.; Jiang, S.-Y.; Zheng, R.-H.; Chen, W. Titanite U-Pb dating and geochemical constraints on the Paleozoic magmatic-metamorphic events and Nb-Ta mineralization in the Yushishan deposit, South Qilian, NW China. *Lithos* **2022**, *412–413*, 106612. [[CrossRef](#)]
44. Agangi, A.; Kamenetsky, V.S.; Hofmann, A.; Przybyłowicz, W.; Vladýkin, N.V. Crystallisation of magmatic topaz and implications for Nb-Ta-W mineralisation in F-rich silicic melts—The Ary-Bulak ongonite massif. *Lithos* **2014**, *202*, 317–330. [[CrossRef](#)]
45. Vasyukova, O.; Williams-Jones, A.E. Fluoride–silicate melt immiscibility and its role in REE ore formation: Evidence from the Strange Lake rare metal deposit, Québec-Labrador, Canada. *Geochim. Cosmochim. Acta* **2014**, *139*, 110–130. [[CrossRef](#)]
46. Hao, J.; Wang, E.Q.; Liu, X.H.; Sang, H.Q. Jinyanshan collisional orogenic belt of the early Paleozoic in the Altun Tagh mountains: Evidence from single zircon U-Pb and $^{40}\text{Ar}/^{39}\text{Ar}$ isotopic dating for the arc magmatite and ophiolitic mélange. *Acta Petrol. Sin.* **2006**, *22*, 2743–2752, (In Chinese with English Abstract). [[CrossRef](#)]
47. Jia, Q.Z.; Yang, Z.T.; Xiao, Z.Y.; Quan, S.C.; Zou, X.H.; Xiao, S.Y.; Wang, S.Q.; Li, B.Q.; Li, B.X.; Wu, Y.Z.; et al. *Metallogenetic Regularity and Metallogenetic Prediction of Qilian Mountain Cu-Au-W-Pb-Zn Deposit*; Geological Publishing House: Beijing, China, 2007; pp. 1–313, (In Chinese with English Abstract).
48. Liu, T.; Jiang, S.Y.; Zheng, R.H.; Chen, W. A discussion on the structure and tectonic evolution of the Altyn Taghorogenic Zone. *Earth Sci. Front.* **2000**, *7*, 206. [[CrossRef](#)]
49. Liu, L.; Zhang, A.D.; Chen, D.L.; Yang, J.X.; Luo, J.H.; Wang, C. Implications based on LA-ICP-MS zircon U-Pb ages of eclogite and its country rock from Jianguozi area, Altyn Tagh. *Earth Sci. Front.* **2007**, *14*, 98–107, (In Chinese with English Abstract). [[CrossRef](#)]
50. Liu, Y.S.; Yu, H.F.; Xin, H.T.; Lu, S.N.; Xiu, Q.Y.; Li, Q. Tectonic units division and Precambrian significant geological events in Altyn Tagh Mountain, China. *Geol. Bull. China* **2009**, *28*, 1430–1438, (In Chinese with English Abstract). [[CrossRef](#)]
51. Yu, S.; Zhang, J.; del Real, P.G.; Zhao, X.; Hou, K.; Gong, J.; Li, Y. The Grenvillian orogeny in the Altun-Qilian-North Qaidam mountain belts of northern Tibet Plateau: Constraints from geochemical and zircon U-Pb age and Hf isotopic study of magmatic rocks. *J. Asian Earth Sci.* **2013**, *73*, 372–395. [[CrossRef](#)]
52. Li, B. *Study on the Early Paleozoic Tectonic Evolution and Cenozoic Intracontinental Development of the Qilian Orogen, Northern Tibet*; Chinese Academy of Geological Sciences: Beijing, China, 2020; (In Chinese with English Abstract). [[CrossRef](#)]
53. Qin, Y. *Neoproterozoic to Early Paleozoic Tectonic Evolution in the South Qilian Orogen*; Northwestern University: Evanston, IL, USA, 2018; (In Chinese with English Abstract).
54. Song, S.; Niu, Y.; Su, L.; Zhang, C.; Zhang, L. Continental orogenesis from ocean subduction, continent collision/subduction, to orogen collapse, and orogen recycling: The example of the North Qaidam UHPM belt, NW China. *Earth Sci. Rev.* **2014**, *129*, 59. [[CrossRef](#)]
55. Tung, K.-A.; Yang, H.-Y.; Liu, D.-Y.; Zhang, J.-X.; Yang, H.-J.; Shau, Y.-H.; Tseng, C.-Y. The Neoproterozoic granitoids from the Qilian block, NW China: Evidence for a link between the Qilian and South China blocks. *Precambrian Res.* **2013**, *235*, 163–189. [[CrossRef](#)]
56. Guo, N.X.; Liu, S.B.; Chen, Z.Y.; Jiang, S.X.; Li, H.W. Mechanism of Nb and REE enrichment in the Tiemuli alkali feldspar granite, Chongyi County, Jiangxi Province. *Acta Petrol. Sin.* **2022**, *38*, 371–392, (In Chinese with English Abstract). [[CrossRef](#)]
57. Wang, K.; Wang, L.-X.; Ma, C.-Q.; Zhu, Y.-X.; She, Z.-B.; Deng, X.; Chen, Q. Mineralogy and geochemistry of the Zhuxi Nb-rich trachytic rocks, South Qinling (China): Insights into the niobium mineralization during magmatic-hydrothermal processes. *Ore Geol. Rev.* **2021**, *138*, 104346. [[CrossRef](#)]
58. Zhao, Z.; Yang, X.; Lu, S.; Lu, Y.; Sun, C.; Chen, S.; Zhang, Z.; Bute, S.I.; Zhao, L. Genesis of Late Cretaceous granite and its related Nb-Ta-W mineralization in Shangbao, Nanling Range: Insights from geochemistry of whole-rock and Nb-Ta minerals. *Ore Geol. Rev.* **2021**, *131*, 103975. [[CrossRef](#)]
59. Li, X.-H.; Li, W.-X.; Li, Q.; Wang, X.-C.; Liu, Y.; Yang, Y.-H. Petrogenesis and tectonic significance of the 850 Ma Gangbian alkaline complex in South China: Evidence from in situ, zircon U-Pb dating, Hf-O isotopes and whole-rock geochemistry. *Lithos* **2010**, *114*, 1–15. [[CrossRef](#)]
60. Song, S.; Su, L.; Li, X.-H.; Zhang, G.; Niu, Y.; Zhang, L. Tracing the 850 Ma continental flood basalts from apiece of subducted continental crust in the North Qaidam UHPM belt, NW China. *Precambrian Res.* **2010**, *183*, 805–816. [[CrossRef](#)]

61. Chen, H.J. *Petrogenesis and Continental Dynamic Significance of the Neoproterozoic Granitoids in the Altyn Tagh*; China University of Geosciences: Beijing, China, 2018; (In Chinese with English Abstract).
62. Hao, J.B. *Composition, Geochronology and Mesoproterozoic-Neoproterozoic Tectonic Evolution of the Central-Southern Altyn Tagh*; Northwestern University: Evanston, IL, USA, 2021; (In Chinese with English Abstract).
63. Li, H.K.; Lu, S.N.; Wang, H.C.; Xiang, Z.Q.; Zheng, J.K. Geological record of Neoproterozoic supercontinent cracking in the northern margin of Qaidam, Qinghai Province: Quanji Group. Geological survey and Research. *Geol. Surv. Ang Res.* **2003**, *26*, 27–37, (In Chinese with English Abstract).
64. Liu, Y.S.; Xin, H.T.; Zhou, S.J.; Teng, X.J.; Yang, J.Q.; Lv, H.Q. *Precambrian and Paleozoic Tectonic Evolution of Lapaiquan Area Ineastern Altun Tagh Mountains*; Geological Publishing House: Beijing, China, 2010; pp. 155–156. (In Chinese)
65. Wu, R.-X.; Zheng, Y.-F.; Wu, Y.-B.; Zhao, Z.-F.; Zhang, S.-B.; Liu, X.; Wu, F.-Y. Reworking of juvenile crust: Element and isotope evidence from Neoproterozoic granodiorite in South China. *Precambrian Res.* **2006**, *146*, 179–212. [[CrossRef](#)]
66. Zhang, J.X.; Yang, J.S.; Meng, F.C.; Wan, Y.S.; Li, H.M.; Wu, C.H. U–Pb isotopic studies of eclogites and their host gneisses in the Xitieshan area of the North Qaidam Mountains, western China: New evidence for an early Paleozoic HP-UHP metamorphic belt. *J. Asian Earth Sci.* **2006**, *28*, 143–150. [[CrossRef](#)]
67. Shi, R.D.; Yang, J.S.; Wu, C.L. The discovery of adakitic dacite in Early Palaeozoic island arc volcanic rocks on the northern margin of Qaidam basin and its geological significance. *Acta Petrol. Miner.* **2003**, *22*, 229–236, (In Chinese with English Abstract). [[CrossRef](#)]
68. Shi, R.D.; Yang, J.S.; Wu, C.L.; Tsuyoshi, I.; Takafumi, H. Island arc volcanic rocks in the north Qaidam UHP belt, northern Tibet plateau: Evidence for ocean-continent subduction preceding continent-continent subduction. *J. Asian Earth Sci.* **2006**, *28*, 151–159. [[CrossRef](#)]
69. Wang, H.C.; Lu, S.N.; Yuan, G.B.; Xin, H.T.; Zhang, B.H.; Wang, Q.H.; Tian, Q. Tectonic properties and formation age of Tanjian Mountain Group in the northern margin of Qaidam Basin. *Geol. Bull. China* **2003**, *22*, 487–493, (In Chinese with English Abstract). [[CrossRef](#)]
70. Wu, C.L.; Yang, J.S.; Xu, Z.Q.; Joseph, L.W.; Trevor, I.; Li, H.B.; Shi, R.D.; Meng, F.C.; Chen, S.Y.; Harold, P.; et al. Granitic magmatism in the Paleozoic ultra-high pressure zone in the northern margin of Qaidam Basin. *Acta Geol. Sin.* **2004**, *78*, 658–674, (In Chinese with English Abstract). [[CrossRef](#)]
71. Zhang, J.X.; Meng, F.; Yu, S.Y. Two contrasting HP/LT and UHP metamorphic belts: Constrainton Early Paleozoic orogeny in Qilian-Altunorogen. *Acta Petrol. Sin.* **2010**, *26*, 1967–1992.
72. Song, S.; Niu, Y.; Su, L.; Xia, X. Tectonics of the north Qilian orogen, NW China. *Gondwana Res.* **2013**, *23*, 1378–1401. [[CrossRef](#)]

Disclaimer/Publisher’s Note: The statements, opinions and data contained in all publications are solely those of the individual author(s) and contributor(s) and not of MDPI and/or the editor(s). MDPI and/or the editor(s) disclaim responsibility for any injury to people or property resulting from any ideas, methods, instructions or products referred to in the content.